lubricants

MDPI

Supporting Information

Nanocomposite of Poly(L-lactic acid) with inorganic nanotubes of WS_2

Hila Shalom[1], XiaoMeng Sui[1], Olga Elianov[1], Vlad Brumfeld[2], Rita Rosentsveig[1], Iddo Pinkas[2], Yishay Feldman[2], Nir Kampf[1], H.D. Wagner[1], Noa Lachman[3], Reshef Tenne[1]

[1] Department of Materials and Interfaces, Weizmann Institute, Rehovot 76100, Israel;
[2] Department of Chemical Research Support, Weizmann Institute, Rehovot 76100, Israel;
[3] Department of Materials Science and Engineering, Faculty of Engineering, Tel-Aviv University, Ramat Aviv, Tel Aviv 6997801, Israel
* Correspondence: reshef.tenne@weizmann.ac.il; Tel.: +972-8-9342394

Received: date; Accepted: date; Published: date

3. Results and discussion

Fig. S1 reports the weight loss of the films annealed at 30 °C under vacuum for one week.

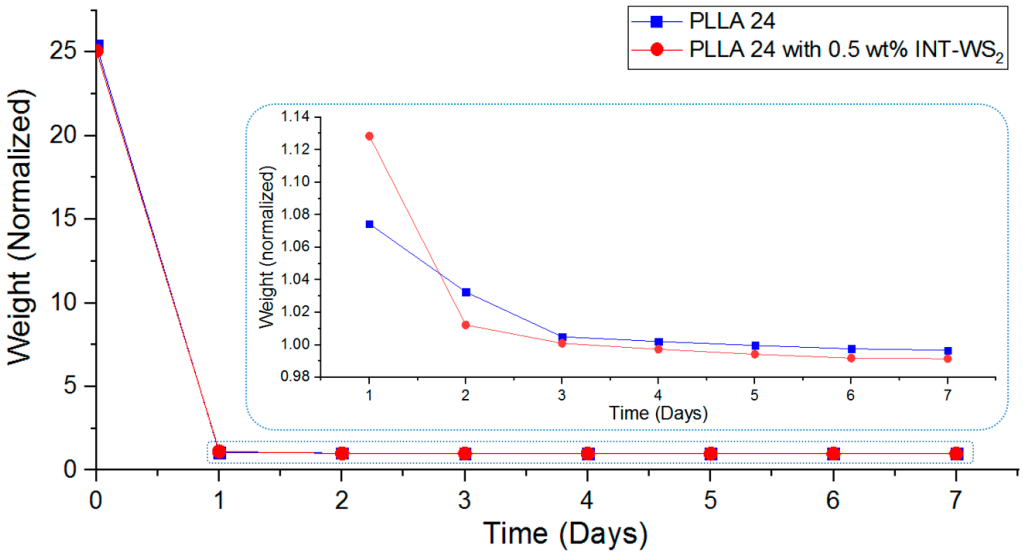

Fig. S1. Weight loss of the PLLA 24 films during annealing at 30 °C under vacuum for one week.

3.3. X-ray Tomographic Microscopy (Micro-XCT)

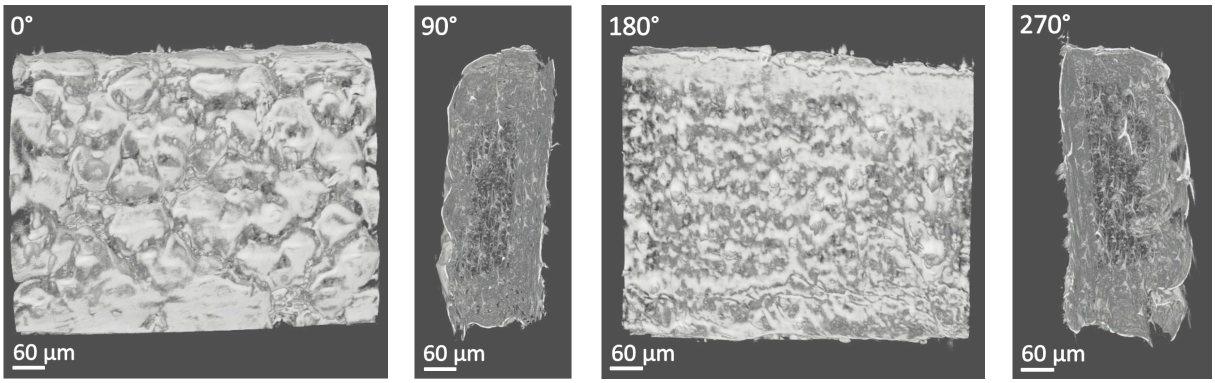

Fig. S2. Images from 360° revolution of the film (sample No. 2 in Table 3) obtained by micro-XCT after tensile test in the neck zone near the fracture point. Please note that the sample width is reduced compared to the untested sample, which is clearly visible in 90 and 270°. Furthermore, the nanotubes are visibly oriented in these cross-section views.

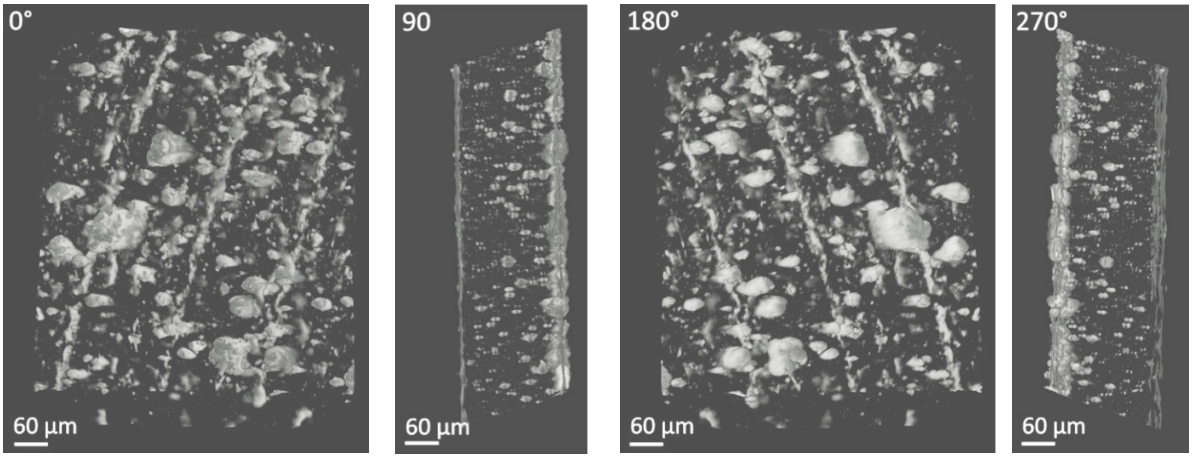

Fig. S3. Images from 360° video in the micro-XCT of PLLA 38 film with 1 wt% INT-WS_2 (sample No. 3) before tensile test. The nanotubes are highly agglomerated compared with the 0.5 wt% specimen. Note the difference between the top (thin) and bottom (thick) surfaces of the sample. The stripes appearing in 0 and 180° projections are obtained by the modulated morphology of the Teflon surface

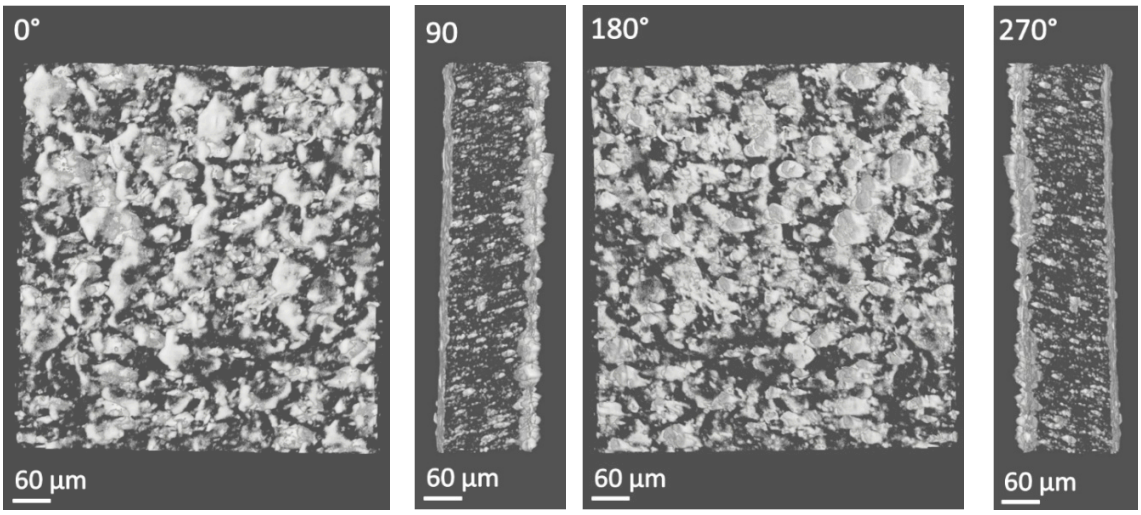

Fig. S4. Images from the 360° video in the micro- XCT of PLLA 38 film with 1 wt% INT-WS_2 (No. 3) after tensile test.

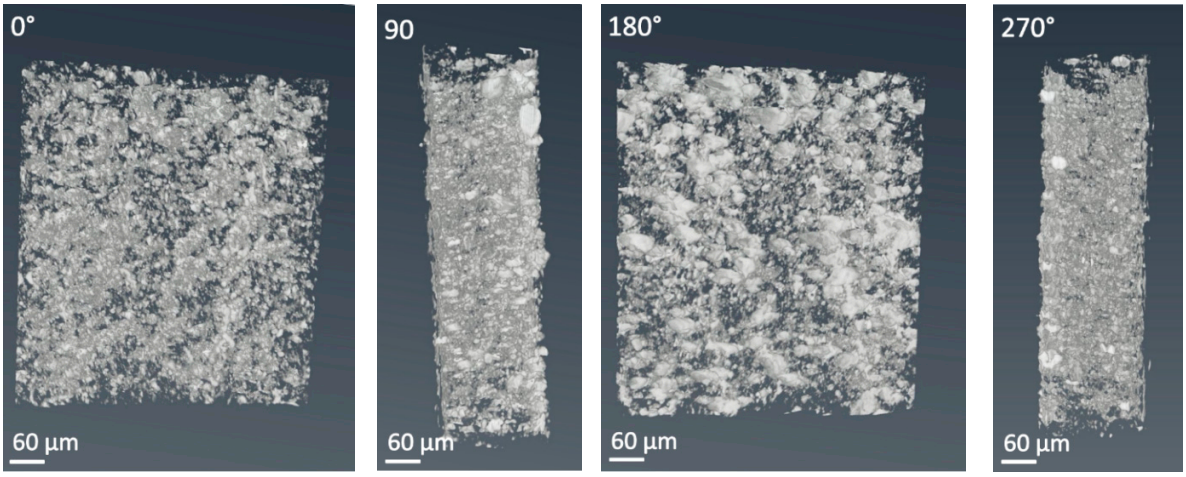

Fig. S5. Images from the 360° video in the micro-XCT of PLLA 38 film with 3 wt% INT-WS_2 (No. 4) before tensile test.

3.2. Functionalization of the INT-WS_2

3.2.2. Functionalization of INT-WS_2 with NMP (N-Methyl-2-pyrrolidone)

NMP has been used in the past to functionalize the surface of CNT as well as a host of other kinds of nanoparticles. Unfortunately, the solubility of the PLLA 38 in NMP is inadequate and furthermore the high boiling point (202 °C) required long annealing periods. SEM analysis of the PLLA 38 film with 1 wt% INT-WS_2 after treatment with NMP is shown in **Fig. S6.** The INT-WS_2 were found to disperse well in the film (**Fig. S6B**), but the morphology of the film with the functionalized nanotubes, showed high surface roughness. **Table S1** displays the mechanical properties of the PLLA 38 films containing different weight percent of INT-WS_2 and after annealing for 6 h in 120 °C. The PLLA with NMP-treated tubes showed improved ductility and toughness compared to the neat PLLA, but reduced modulus and strength. Annealing the films at 120 °C

resulted in improved strength up to 130% compared to the blank PLLA 38. However, the ductility of the specimen went down, substantially due to the surface roughening, see **Fig. S6A.** The NMP facilitates the dispersion of the nanotubes thereby improving the ductility and toughness of the PLLA with NMP-treated tubes. However, the strength of the nanocomposite was reduced in comparison to the neat PLLA 38. In contrast, the annealed PLLA films showed the opposite phenomenon presenting improved modulus and strength but reduced ductility and toughness.

The inability of NMP to dissolve PLLA, suggests that the adhesion of the NMP-treated tubes to the polymer matrix was quite poor, which explained the reduced ductility of the nanocomposites. The annealing helped to improve the mechanical properties of the neat PLLA by evaporating the remainder of the solvent molecules. Furthermore, the annealing of the composite film, enhanced the initially poor compatibility of the NMP-treated tubes to the polymer matrix, by increasing the compactness of the PLLA and NMP/nanotubes matrix.

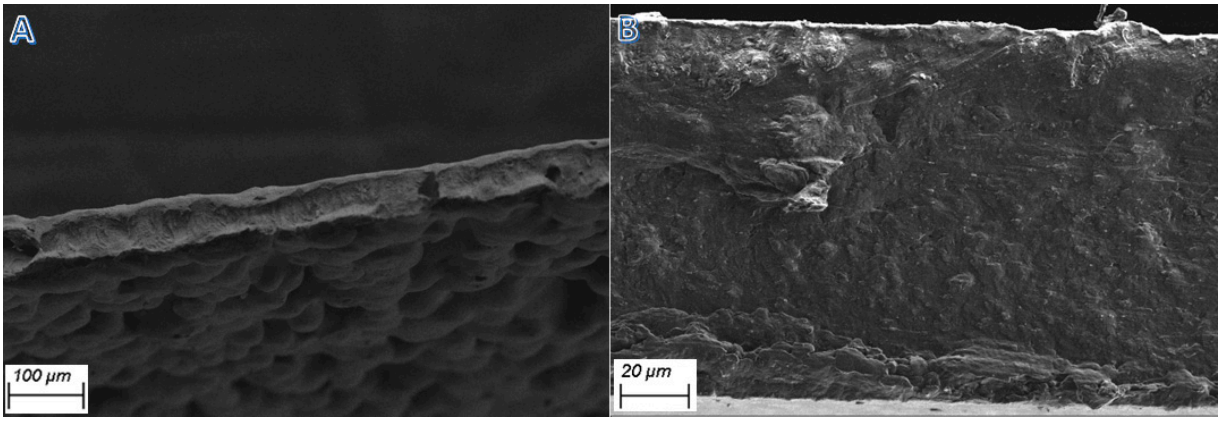

Fig. S6. SEM images of: A - PLLA 38 film with 1 wt% INT-WS_2 after treatment with NMP and vacuum annealing for 6 h in 120°C; B – magnified image of the cross-section of the film.

Table S1: Mechanical properties of - PLLA 38 film with INT-WS_2 after treatment with NMP.

	Modulus (GPa)	**Yield strength (MPa)**	**Elongation (%)**	**Toughness (MPa*%)**	**Thickness (mm)**
PLLA 38 film	1.5±0.05	41.9±10.9	1.5±0.6	0.6±0.05	0.15±0.1
PLLA 38 film with 0.25 wt% INT-WS_2 after functionalized with NMP	1.75±0.05	38.0±1.6	10.4±1.6	7.9±2.2	0.12±0.1
PLLA 38 film with 0.5 wt% INT-WS_2 after functionalized with NMP	1.4±0.02	31.7±2.3	9.5±2.1	2.4±0.6	0.12±0.1
PLLA 38 film with 1 wt% INT-WS_2 after functionalized with NMP	1.4±0.3	67.4±48.9	15.4±1.3	3.9±0.3	0.15±0.1
PLLA 38 film after vacuum annealing for 6 h in 120°C	1.9±0.2	51.5±2.4	7.2±1.6	2.4±0.2	0.13±0.1
PLLA 38 film with 0.25 wt% INT-WS_2 after functionalized with NMP and after vacuum annealing for 6 h in 120°C	2.1±0.2	38.9±0.5	3.3±0.2	0.8±0.1	0.13±0.1
PLLA 38 film with 0. 5 wt% INT-WS_2 after functionalized with NMP and after vacuum annealing for 6 h in 120°C	2.3±0.05	56.4±1.0	3.8±1.1	1.1±0.4	0.2±0.1

3.2.3. Functionalization of INT-WS_2 with PEG (Polyethylene glycol)

The mechanical properties of PLLA 24 film with different concentrations of INT-WS_2 after functionalization with PEG are shows in **Table S2**. Both strength and ductility of the films with nanotubes were improved after functionalization in all weight percentages. As the concentrations of the nanotubes increased, the ductility of the film improved first. Further increase of the nanotube concentration led also to improvements in the strength. The largest improvement was obtained around 0.5 wt% INT-WS_2 (by 150% compared to the neat PLLA). Similar trend was observed for the polymer films with nanotubes after functionalization in PEI. The minor improvement in the mechanical properties compared to the neat nanotubes could be due the reorientations of the nanotubes in the tensile direction.

Table S2: Mechanical properties of PLLA 24 film with INT-WS_2 after treatment with PEG.

	Modulus (GPa)	Yield strength (MPa)	Elongation (%)	Toughness (MPa*%)	**Thickness (mm)**
PLLA 24 film	1.3±0.1	22.3±1.8	2.9±0.7	0.4±0.1	0.13±0.1
PLLA 24 film with 0.25 wt% INT-WS_2	1.8±0.05	41.5±1.4	8.1±1.5	2.0±0.4	0.11±0.1
PLLA 24 film with 0.5 wt% INT-WS_2	2.8±0.2	60.9±2.8	18.4±5.2	5.7±0.7	0.10±0.1
PLLA 24 film with 0.8 wt% INT-WS_2	2.2±0.2	43.7±3.5	10.3±2.4	3.8±1.2	0.10±0.1
PLLA 24 film with 0.25 wt% INT-WS_2 after functionalized with PEG	1.9±0.05	28.6±1.8	9.1±1.3	1.8±0.6	0.12±0.1
PLLA 24 film with 0.5 wt% INT-WS_2 after functionalized with PEG	1.9±0.3	40.6±7.6	10.0±5.1	1.8±0.5	0.12±0.1
PLLA 24 film with 1 wt% INT-WS_2 after functionalized with PEG	2.0±0.05	34.8±1.0	2.9±0.2	0.7±0.1	0.14±0.1

3.4. Differential scanning calorimetry (DSC)

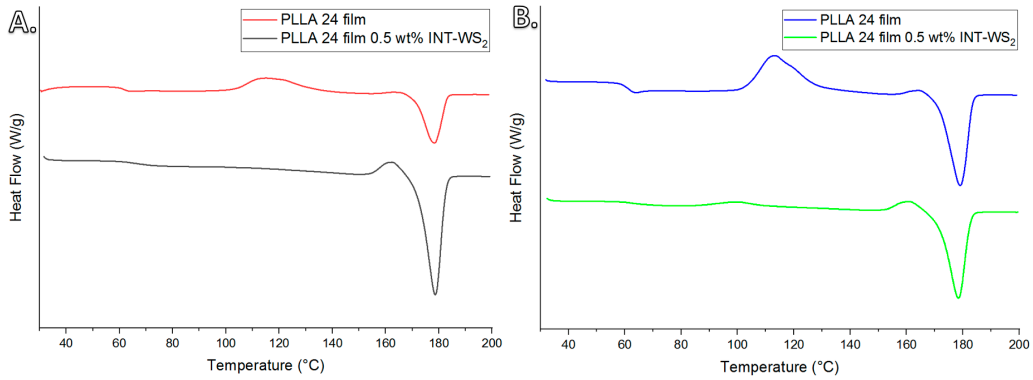

Fig. S8. DSC melting thermograms of PLLA 24 neat and with 0.5 wt% INT-WS_2 (A) immediately after preparation and (B) after one year.

3.5. X-ray Diffraction

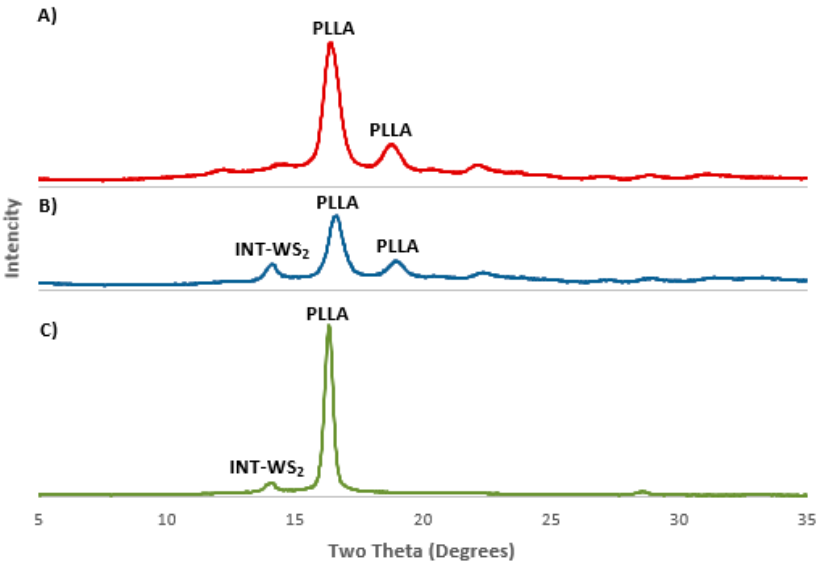

Fig. S8. XRD patterns of (A) PLLA 38 film, (B) PLLA 38 film with 1 wt% INT-WS_2 (C) PLLA 38 wires with 1 wt% INT-WS_2.

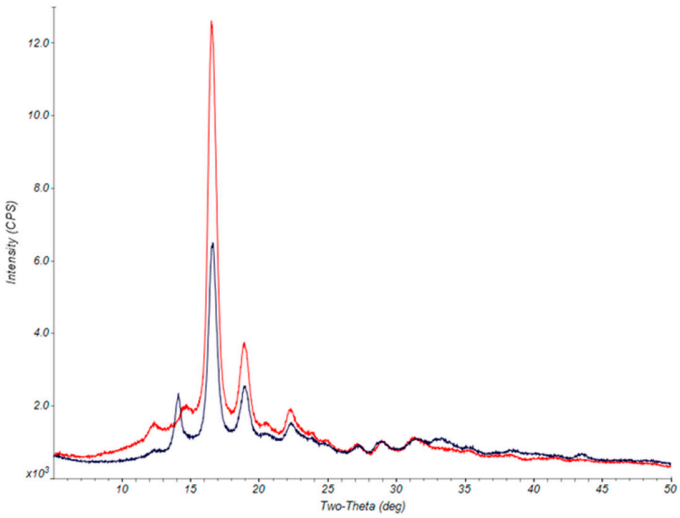

Fig. S9. XRD patterns of (A) PLLA 38 film (red) and (B) PLLA 38 film with 1 wt% INT-WS_2 (black)

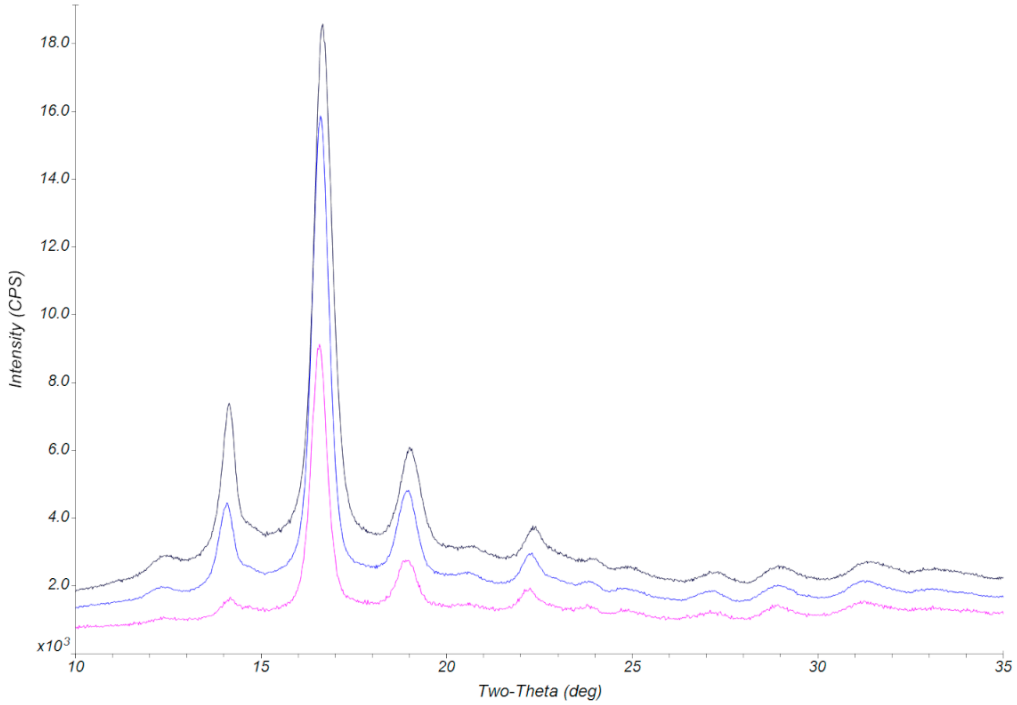

Fig. S10. XRD pattern of the PLLA 24 specimen with 0.5 wt% INT-WS_2 immediately after preparation (black curve), and the same sample one year later. The sample was studied from both sides: back surface (blue curve) and front surface (purple curve).

3.6. Friction force

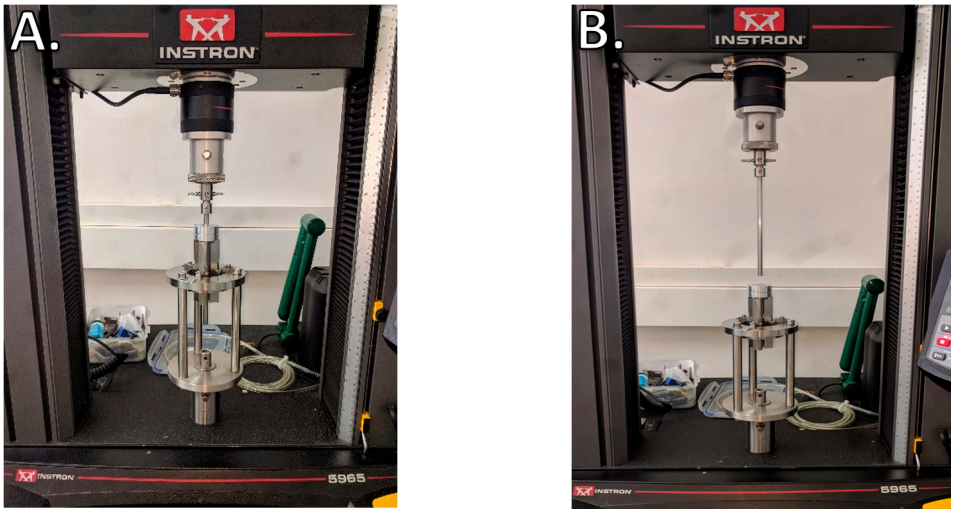

Fig. S11. Pictures of the modified mock-up model of the urethra–endoscope (UM model) pair mounted on the Instron and attached to the load cell A. The stainless steel (uncoated) rod is inserted to the RTV ring, which is fixed between two circular metal pieces. B. The stainless steel (uncoated) rod is outside the UM.

3.7. Raman spectroscopy

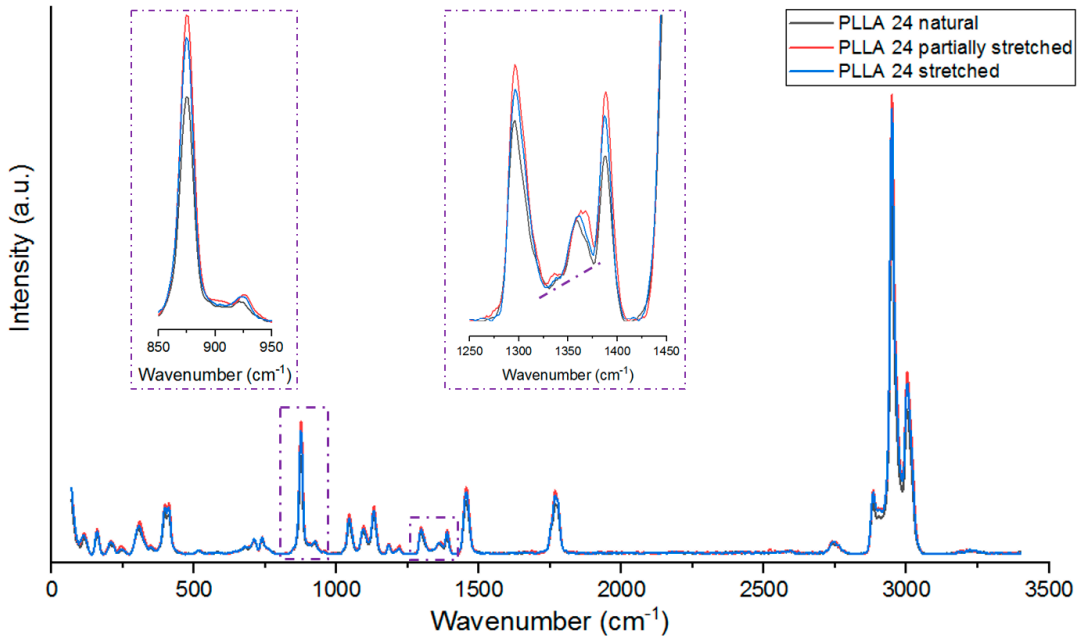

Fig. S12. Raman spectra of PLLA 24 film before (natural) and after tensile test (partially stretched and stretched). Inset: Raman spectra in 850-950 cm^{-1} and 1250-1450 cm^{-1} regions. The dashed line represents the slope between 1250-1450 cm^{-1} bands of PLLA.

The Raman spectra presented a shoulder line at 923 cm^{-1} next to a strong Raman line at 873 cm^{-1} (see inset of **Fig. S12**), which is associated with the semi-crystalline PLLA phase [47,48]. Several bands were observed in the region 1250-1450 cm^{-1}. The 1293 cm^{-1} band was assigned to the δ_2CH IR bending mode; the 1363 cm^{-1} peak to the δ_1CH bend and the 1388 cm^{-1} peak to the δ_sCH3 bend. The slop between those bends (see also the inset to **Fig. S12**) is associated also with the semi-crystalline nature of the PLLA phase [47,48]. Therefore, it can be concluded that the PLLA matrix is semi-crystalline and does not contain amorphous phase to any significant extent.

The Raman spectra for PLLA 24 with 0.5 wt% of INT-WS_2 before and after tensile test (**Table 3**, No. 6), are displayed in **Fig. S13**. There is a slight difference in the composition of the specimen due to the presence of the nanotubes and the stretching of the specimen. First, the lines at 350 and 420 cm^{-1} are associated with the presence of the WS_2 nanotubes in the poymer matrix [49]. The nanocomposite is also semicrystalline (see the shoulder in 923 cm^{-1} and the slope between the bonds in 1250-1450 cm^{-1} region in the inset to **Fig. S13**).

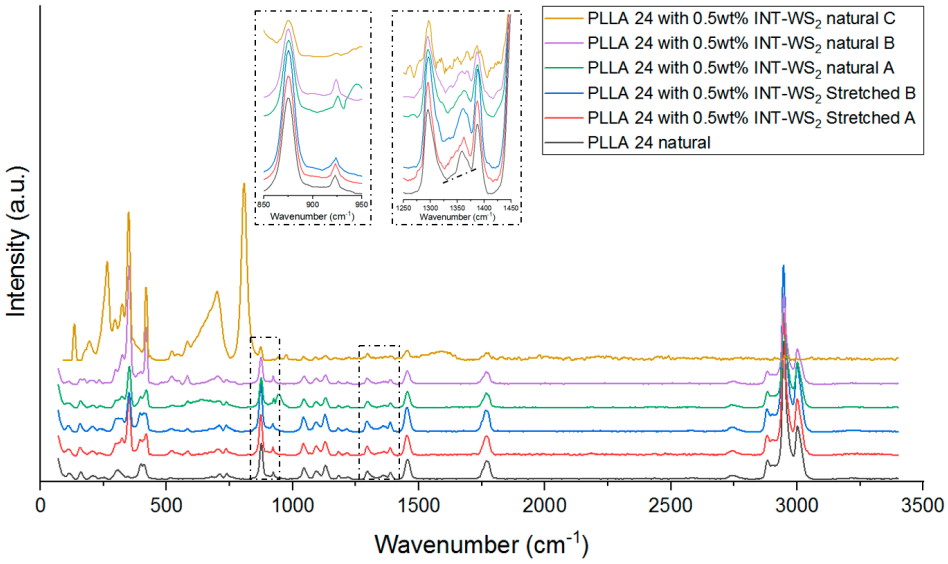

Fig. S13. Raman spectra of PLLA 24 film (natural) and with 0.5 wt% INT-WS_2 (natural), before and after tensile test (stretched) taken in two different spots. The dashed line represents the slope between 1250-1450 cm^{-1} bands of PLLA.